SURFACE STRUCTURE, COMPOSITION AND HARDENABILITY OF CU-10NI-2AL ALLOY DEVELOPED IN A MAGNETRON SPUTTERING SYSTEM

HANY NAZMY SOLIMAN & ATEF RIZK

Physics Department, Faculty of Education, Ain Shams University, Roxy, Cairo, Egypt

ABSTRACT

Experiments have been made to examine changes in surface structure and composition as well as hardenability of the Cu-10Ni-2Al alloy due to different treatments in argon magnetron sputtering and different heat treatments. Furthermore, hysteresis behaviour of the given alloy in dry argon atmosphere at two different gas pressures was investigated. The results showed that sputtering times and annealing temperatures were greatly affected these changes. Presence of aluminum in the alloy was found to increase its hardness compared to that of the Cu-10Ni alloy. Scanning electron microscopy, X-ray diffraction, energy-dispersive X-ray spectroscopy as well as Vickers microhardnesstester were used in this study.

KEYWORDS: Cu-Ni-Al Alloys, Surface Structure, Magnetron Sputtering;Energy DispersiveSpectroscopy, Vickers Hardness

INTRODUCTION

Cu-Ni alloys are single phased throughout the full range of compositions and many standard alloys exist within this range, usually with small additions of other elements used for special purposes[1]. Cu-Ni alloys have interesting physical and mechanical properties, even under continuous loading and at elevated temperatures, together with high resistance to corrosion in many media. Therefore, they are widely used in metallurgical works andmarine environments [2,3].For most applications, the Cu-10Ni alloy is more widely used in marine industry which provides good service at a lower cost [4,5].On the other hand, the properties of the binary Cu-10 Nialloy are not adequate for many applications. Certain properties of this alloy can be significantly improved by adding several elements.Among these elements, aluminium, iron, tin, niobium, silicon,chromium, beryllium and manganese are technically important[6-15].

High strength copper alloys play a significant role in the automation industry, and automobile industry, as well as electrical and electronicsindustry[16,17].Cu–Be alloys are the most widely used elastic copper, owing to their high strength and electrical conductivity[18].However, the high toxicity of beryllium in Cu–Be alloys limits their processing and application. Many researchers have put great effort to develop new elastic copper alloys without beryllium, such asCu–Ni–Al alloys to replace the harmful Cu–Be alloys[19].The principle high strength Cu-Ni-Al alloys result from the fact that the presence of aluminiumin these alloys increases the strength through the formation of age-hardening precipitates, principally consisting of Ni_3Al (known as gamma prime) [20]. Recently, the authors have made a study on the effects of physical sputtering and annealing temperature on surface behaviourof Cu-10Ni alloyand showed that surface topography and composition of this alloy as well as its hardness were greatly affected by sputtering time and annealing temperature[21]. Accordingly, it was considered useful to fulfil previous studies and investigate the effects of Al addition

on sputtering characteristics, surface compositionand hardenability of the Cu-10Ni alloy.

EXPERIMENTAL PROCEDURES

Materials and Samples Preparation

The Cu-10Ni-2Al alloy used in the present study was prepared from predetermined weights of spectroscopically pure copper, nickel and aluminiummetals. The method of preparation was described elsewhere [22].Homogenization was achieved by solutionizing the in got at 873 K for 24 h. The ingot was then cold rolled at a 10% reduction per pass to a final thickness of 0.25 mm with intermediate steps of annealing during the rolling process. The elemental composition of the alloy under investigation was obtained as Cu-10.5wt.%Ni-1.9wt.%Al by using energy-dispersive X-ray spectrometer. Figure. 1 shows the presence of Cu, Ni and Al elements in the as-received sample. Samples undergoing the previous steps were polished to obtain the as-received material and some of them were transferred to a furnace for various heat treatments as will be explained below.
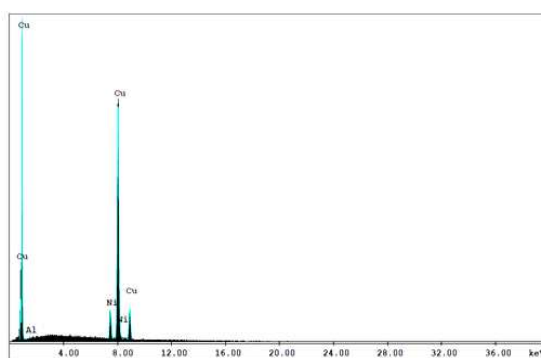

Figure 1: EDX Spectrum Showing the Different Elements in the Cu-10Ni-2Al Alloy

Experimental Methods

Samples of the Cu-10Ni-2Al alloy (1.5 cm × 0.5 cm) were cut and annealed in groups in the temperature range (473-1073 K) for 1 h followed by water quenching. All samples were electopolished to be ready for different analyses, measurements and examinations.The hardnessof this alloy wastestedby Vickers microhardness tester (Model MHP 160) under the load of 80gf for 30 s. At least 15 indentations for each sample were considered to obtain accurate results. Scanning electron micro scopy equipped with an energy-dispersive X-ray spectrometer (EDS/EDAX Genesis FESEM/ QUANTAFEG 250, Central Metallurgical Research and Development Institute, El Tabbin, Cairo–Egypt)was used to examine the changes in surface topographies of the alloy samplesas well as their surface compositions due to ionic bombardment.

Additionally, phase analysis of the samples before and after the different annealing treatments was performed using X-ray diffractometry (Philips X' Pert Multi Purpose Diffraction Diffractometer) and filtered CuKα radiation with a wavelength of 1.5406Å was used. The X-ray diffraction (XRD) patterns overa wide range of diffraction angles 2θ ranging from 30◦ to 100◦ were recorded at room temperature.On the other hand, sputtering experiments were performed using a d.c. magnetron sputtering system (Balzers SCD 040) which has been described in detail elsewhere [23]. A Cu-10Ni-2Al disc of 54 mm diameter and 0.25 mm thickness was used as a targetand formed the outer face of the water-cooled cathode and the small cut samples (1.5 cm × 0.5 cm) were fixed on the target. The vacuum system was pumped downto an ultimate

pressure of 10^{-3} mbar before gas admission using a two-stage rotary pump with a pumping speed of 4 m^3/h. Argon gas of 99.999% purity was employed to the vacuum system through a copper coil immersed in liquid nitrogen, before admission to the vessel, to remove water vapour and P_2O_5 was used as a drying agent inside the vessel.All sputtering experiments were carried out in an argon atmosphere, gas pressure of 0.1mbar and constant input power of about 21 W. The samples were sputtered separately for different times (1 h, 2 h and 3 h) and the sputtered samples were then examined by both scanning electron microscopy (SEM) and energy dispersive spectroscopy (EDS).

RESULTS AND DISCUSSIONS

Hysteresis Bebaviour

The current–voltage characteristics for the targets depend on several parameters such that current density, ion energy, target's material, gas pressure and gas type. Ion bombardment of the Cu-10Ni-2Al target in a dry gas atmosphere of Ar^+ resulted in the I-V characteristics shown in Figure. 2 (a, b) at two successive gas pressures of P_1(0.05 mbar) and P_2(0.1 mbar). It is interesting to note the formation of hysteresis loops due to the lack of coincidence of the curves for increasing and decreasing voltage. As can be seen from Figure. 2, as the applied voltage was increased,the corresponding current value increased for both gas pressures ($P_1$and P_2). This increase in the current values was expected since the sputtering yield and thus the number of the emitted secondary electrons increases with increasing the applied voltage [24].
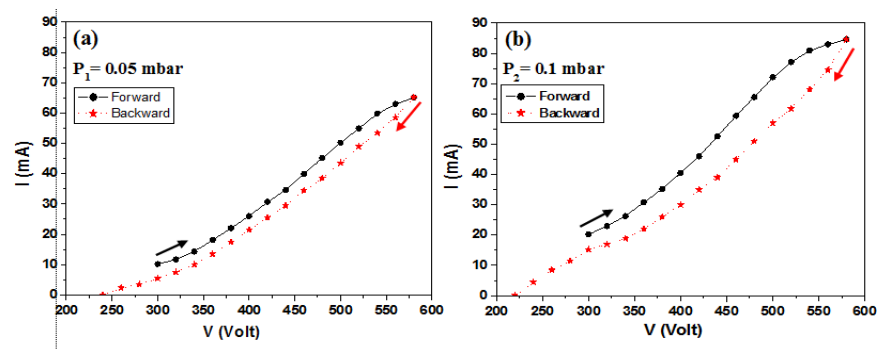

Figure 2: I-V Characteristics of Cu-10Ni-2Al Targets Due to Ar^+ Sputtering at Two Successive Gas Pressures:
(a) 0.05 mbar; (b) 0.1 mbar

From the first insight, one can realize that higher current values are obtained when increasing the gas pressure from P_1 (0.05 mbar) to P_2 (0.1 mbar) at constant applied voltage.This can be understood on the fact that as the gas pressure increases, the number of ions increases in the glow discharge atmosphere causing more atoms to be sputtered off the target with the possibility of more emission of secondary electrons. Since the total current is the algebraic sum of gas ions and emitted secondary electrons, therefore as the gas pressure increases the current increases too.In Figure. 2a, as the applied voltage is decreased rapidly from 580 to 220 V (time taken for the whole hysteresis loop is approximately 3 min), the corresponding current values depart to lower values from those previously obtained during the first path of the cycle. It is believed that the characteristics obtained in this case are based on the formation of thinoxidelayer which redepositson the target surface (during the first path of the cycle) as well as the deionization process of the gas. Thus, because of this oxide layer, more dissipation of the incident ion energy occurs leading to a smaller number of sputtered atoms (i.e., a smaller number of the emitted secondary electrons) and consequently lower current values are obtained. It is also clear from Figure. 2 that the area of the hysteresis loop is related to the gas pressure, it is larger at the higher pressure P_2 (Fig. 2b).

Surface Structure

Sputtering the As-received Samples

It is well known that preferential sputtering of one of the target components leads to the formation of an alternated layer whose composition is different from the bulk.The surface structure of the as-received polished sample is given in Figure. 3a as a reference, and the morphological features developed on surfaces of the sputtered samples for different times (1 h, 2 h and 3 h) are given in Figure. 3(b-d).From the first insight, one can observe that the surface of the as-received (unsputtered) sample appeared almost smooth and free from any isolated particles. As the sample was sputtered for 1 h, the surface became slightly eroded with the appearance of some nano particles (Figure. 3b).As the sputtering time increased to 2 h, the surface became more eroded with the appearance of some large cones (Figure. 3c). Increasing the sputtering time up to 3 h caused the disappearance of most of these cones and the surface appeared fully covered with nano particles (Figure. 3d). Figure. 4 is a higher magnification of Figure. 3 d which shows that the sizes of the different scattered particles that appeared on the surface are on average of 100 nm (nano particles).
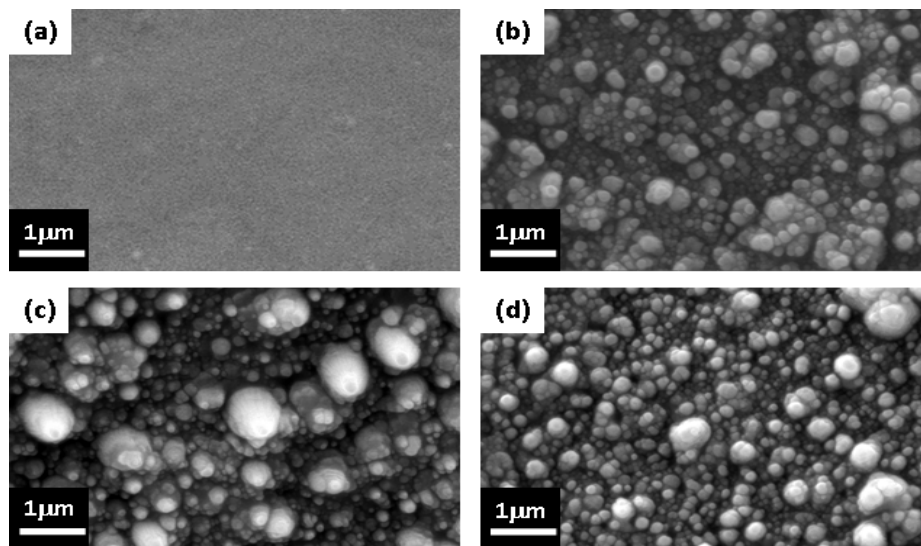

Figure 3: Surface Morphology of the As-received Cu-10Ni-2Al Samples Developed in Ar$^+$ D.C Glow Discharge for: (a) 0 h (Unsputtered), (b) 1 h, (c) 2 h, (d) 3 h (X60 000)
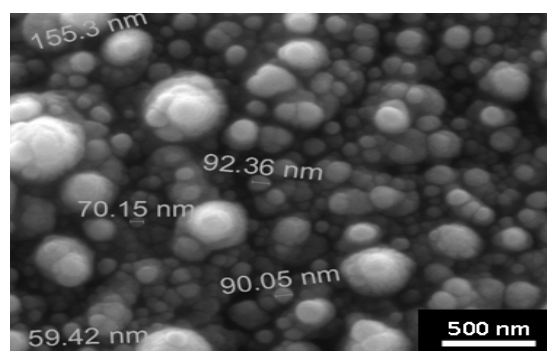

Figure 4: A Higher Magnification of Figure. 3d Showing Different Sizes of Some Scattered Particles.(X100 000)

The cyclic changes of Figure. 3(b-d) can be attributed to the presence of particles with different sputtering yields. As the sputtering time increased to 2 h, some particles (of high sputtering yield) are sputtered off caused partial depletion of the surface from these particles, while other particles (of low sputtering yield) are appeared on the surface as large cones

(Figure. 3c). As the sputtering time increased to 3 h (Figure. 3d), most of these large cones are sputtered off and small particles are appeared again similar to those shown in Figure. 3b.

Sputtering the Annealed Samples

Two groups of samples were annealed for 1 h at two different temperatures 873 K and 1073 K, respectively. These annealed sampleswere then subjected to sputtering process in argon dc glow discharge for 3 h and their surface morphological features are shown in Figure. 5.As shown in Figure. 5a, a rough surface associated with the appearance of some gathered tiny particles and etch pits were observed in the sample annealed at 673 K. As the annealing temperature increased up to 1073 K (Figure. 5b), the surface appeared to be less rough than that in Figure. 5a but fully covered with nano particles indicating a decrease in the surface roughness.
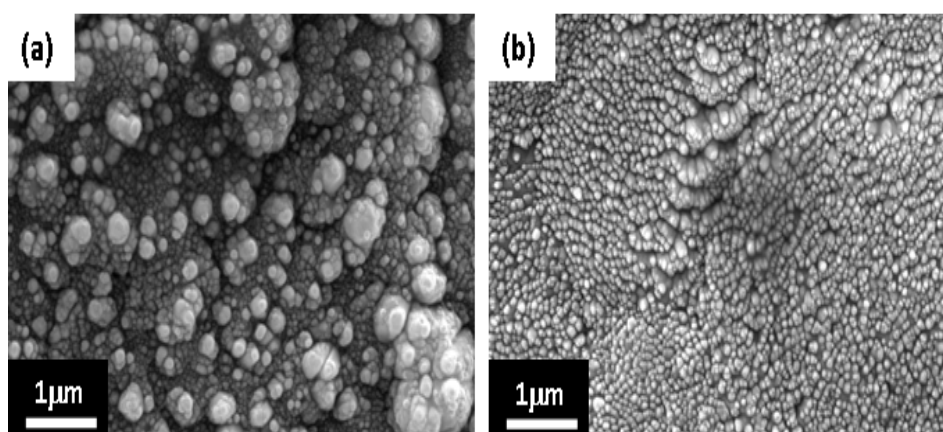

Figure 5: Surface Morphology of the Cu-10Ni-2Al Samples Due To Ar$^+$ Sputtering for 3 h After Annealing the Samples for 1 h at Two Different Temperatures: (a) 673 K; (b) 1073 K.(X60 000)

The XRD analysis given in Figure. 6 (a-c) confirmed the presence of $Cu_{3.8}Ni$ phase.When the samples were annealed at temperatures 673 K and 1073K respectively, Figure. 6 (b, c), a noticeable growth for this phase was observed as compared with that for the as-received sample (Figure. 6a). Furthermore, Figure. 6c shows the disappearance of the CuAl phase and formation of small peaks of Ni_3Al and Al_4Ni_3 phases instead.The growth of the $Cu_{3.8}Ni$ phase associated with increasing the annealing temperature is confirmed by calculating the particle sizefrom the half width of the spectral lines corresponding to this phase using Scherer formula [25].The changes in the average particle size of $Cu_{3.8}Ni$ phase associated with increasing the annealing temperature are represented in Figure. 7. It was observed from Figure. 7 that the particle sizes of $Cu_{3.8}Ni$ phase are on the average of 22 nm for the as-received sample. As annealing temperature increased up to 673 K, the average particle size is slightly increased to be 26 nm. Further increase in annealing temperature up to 1073 K, caused a noticeable increase in the average particle size (44 nm).
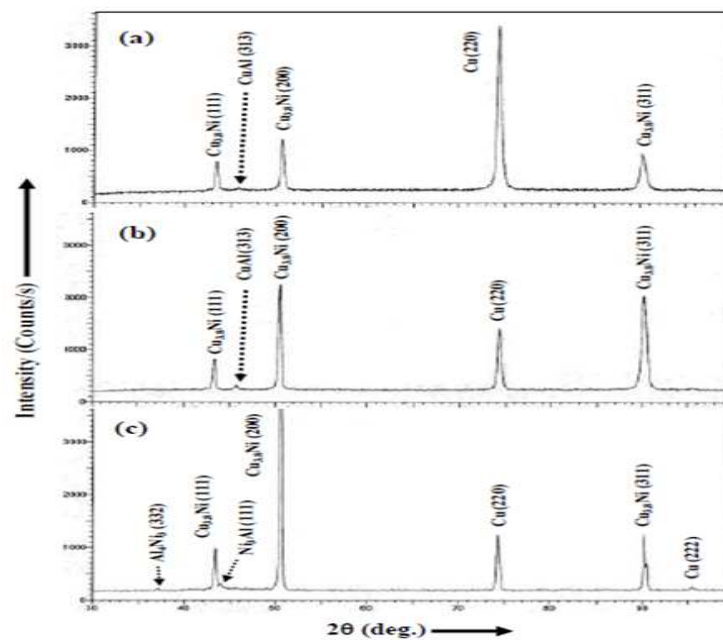
Figure 6: X-Ray Diffraction Patterns Obtained for Cu-10Ni-2Al Samples Annealed for 1 h at Different Temperatures: (a) As-received; (b) 673 K; (c) 1073 K
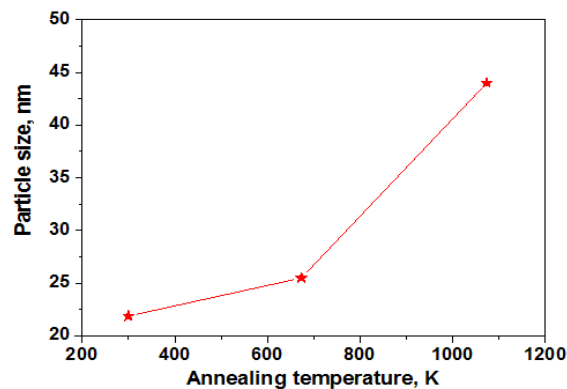

Figure 7: Variation of Average Particle Sizes of the $Cu_{3.8}Ni$ Phase With Annealing Temperature

Elemental Analysis

It is well known that the ion sputtering of multi-element target leads to the preferential sputtering of the elements. So, the surface concentration of the elements after ion sputtering differs from the bulk composition. Spectrum of EDS was used to detect the elemental compositions for the Cu-10Ni-2Al samples before and after the sputtering process. Different zones were selected for each sample and the values of the elemental compositions given in Tables 1, 2 are the average of at least ten measurements. Table 1 gives the elemental compositions for the as-received Cu-10Ni-2Al samples after being sputtered in a dc glow discharge for different times (1 h, 2 h and 3 h). It can be concluded from this Table that increasing the sputtering time up to 3 h resulted in an increase of both Ni and Al contents on the sample surface by approximately 25% and 13%, respectively compared with the unsputtered sample. This is due to the low sputtering yields of both Ni and Al elements compared with that of Cu. The ratio of the sputtering yields of pure Ni and Al with respect to Cu are to be in the form:

$$\frac{Y_{Ni}}{Y_{Cu}} \approx 0.65 \text{ , } \frac{Y_{Al}}{Y_{Cu}} \approx 0.52 \text{ for 500 eV Ar}^+ \text{ bombardment [26].}$$

Table 1: Elemental Compositions for the As-received Cu-10Ni-2Al Samples Sputtered in an Ar$^+$ dc Glow Discharge for Different Sputtering Times

Figure 3	Sputtering Time (h)	% Elemental Composition $\pm$ 0.05			Weight gain percentage of Ni	Weight gain percentage of Al
		wt.%Cu	wt.%Ni	wt.%Al		
(a)	----	87.60	10.50	1.90	----	----
(b)	1	86.96	11.06	1.98	5.3%	4.2%
(c)	2	86.72	11.18	2.10	6.5%	10.5%
(d)	3	84.77	13.08	2.15	24.6%	13.2%

On the other hand, the elemental compositions for the Cu-10Ni-2Al samples being annealed for 1 h at two different annealing temperatures (673 and 1073 K) followed by sputtering in a dc glow discharge for 3 h are given in Table 2. The data in Table 2 showed that sputtering the annealed sample (at 1073 K for 1 h) for 3 h increased the Ni content on the sample surface by approximately 56% compared with the as-received (unsputtered) sample. This increase in the Ni content on the sample surface is referred to: **(i)** the growth of the Cu$_{3.8}$Ni phase particles (Figure. 7) which need more energy to be sputtered off, **(ii)** the fact that surface binding energy of Ni atoms is higher than that of Cu atoms [27]. Moreover, it is well known that the component segregation may result from different diffusion rates between Cu and Ni because the diffusion rate of Cu is faster than that of Ni during annealing process.Therefore, the Cu atoms (of high diffusivity) segregate faster towards the grain boundaries at elevated temperatures and the sample surface becomes enriched with Ni content. This explanation is in accordance with those obtained previously by other authors [28,29].

Table 2: Elemental Compositions for the Cu-10Ni-2Al Samples Being Annealed for 1 h at Two Different Annealing Temperatures (673 K and 1073 K) Followed By Sputtering Separately in an Ar$^+$ dc Glow Discharge for 3h

Figure 5	Annealing Temperature (K)	Sputtering Time (h)	% Elemental Composition $\pm$ 0.05			Weight gain percentage of Ni	Weight loss percentage of Al
			wt.%Cu	wt.%Ni	wt.%Al		
(a)	673	3	86.39	12.06	1.55	15%	18.4%
(b)	1073	3	82.35	16.40	1.25	56.2%	34.2%

Furthermore, Table 2 showed that sputtering the same annealed sample decreased the Al content on the sample surface by approximately 34% compared with the as-received (unsputtered) sample.This decrease in the Al content on the sample surfacemay be attributed to the disappearance of the CuAl phase, besides the thermal energy delivered to Al atoms (of low percentage) during annealing process at elevated temperatures.On the other hand, the remaining Al content on the same sample surface (1.25wt.%) may be due to the formation of both Ni$_3$Al and Al$_4$Ni$_3$ phases which believed to be of low sputtering yields as well.

Increasing the Ni content on the sample surface either due to ion bombardment and/or heat treatment significantly improves the resistance of the given alloy to corrosion in different media[4].

Hardness Measurements

The dependence of Vickers hardness (H_V) on annealing temperaturefor the Cu-10Ni-2Al alloyis plotted in Figure. 8. For the sake of comparison, the H_V values for the binary Cu-10Ni are also included in this figure[21]. It is clear from this figure that H_V values for the Cu-10Ni-2Al samples were always higher than those for the Cu-10Ni. This is believed to be attributed to the addition of Al to the Cu-10Ni alloy which in turn increased its strength by a conventional precipitation hardening mechanism, besides the fact that the anneal hardening effect is more expressive in ternarythan in binary systems [30].Furthermore, Figure. 8 shows that H_V of each alloy decreased slightly with increasing annealing temperature up to 673 K then decreased sharply with further increase in temperature up to 1073 K. The slight decrease in H_V values (for Cu-10Ni-2Al samples) may be attributed to the the partial decrease of crystal imperfections as well as the slight increase in the average particle size of $Cu_{3.8}Ni$ phase from 22 nm to 26 nm as shown in Figure. 7.
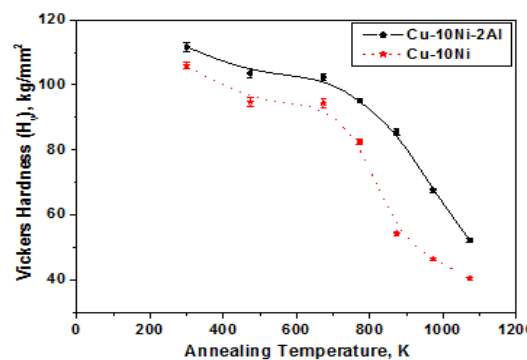

Figure 8: Vickers Hardness Versus Annealing Temperature for Both Cu-10Ni and Cu-10Ni-2Al Alloys

On the other hand, the significant decrease in H_V with increasing annealing temperature above 673 K may be attributed to the reduction of both hardening effect formed previously during cold rolling[31]and/ or density of tiny $Cu_{3.8}Ni$ phase particles (due to their coarsening).Accordingly, one can predicts that above 673 K,the rate of recrystallization of the given alloy increased too and consequently a sharp decrease in H_V values were expected. These results are supported by the data shown in Figure. 7, which shows that the average particle size of $Cu_{3.8}Ni$ phase is significantly increased from 26 nm to 44 nm as the annealing temperature increased from 673 K to 1073 K, respectively.

CONCLUSIONS

Surface structure, composition and hardenability of Cu-10Ni-2Al alloy developed in a magnetron sputtering system were conducted. The main conclusions were drawn as follows:

- Sputtering the as-received Cu-10Ni-2Al sample up to 3 h increased the Ni and Al contents on the sample surface by approximately 25% and 13%, respectively compared with the unsputtered sample.

- Sputtering the annealed Cu-10Ni-2Al sample (up to 1073 K for 1 h) for 3 h increased the Ni content on the sample surface by approximately 56% while decreased the Al content by nearly 34% compared with the as-received (unsputtered) sample.

- Sputtering the annealed sample at a low temperature (673 K) produced rough surface, while sputtering the annealed sample at an elevated temperature (1073 K) provided nearly smooth surface.

- Hardness of the given alloy is found to be dependent on the annealing temperature.

- The presence of Al element in the present alloy is of a major role in increasing material hardness.

REFERENCES

1. Brandes EA.Smithells Metals Reference Book, Sixth Edition, Butterworth & Co 1983

2. Yuan SJ, Pehkonen SO. Surface characterization and corrosion behavior of 70/30 Cu–Ni alloy in pristine and sulfide-containing simulated seawater, Corrosion Science. 2007; 49: 1276–1304.

3. Robert JKW.Erosion–corrosion interactions and their effect on marine and offshore materials. Wear 261. 2006; 1012–1023.

4. Powell C,Webster P. Copper Alloys for Marine Environments, Copper Development Association CDA Publication no 206.2012;p.7.

5. Tharamani CN, Mayanna SM. Low cost black Cu-Ni alloy coating for solar energy applications, Solar Energy Materials & Solar Cells.2007; 91: 664-669.

6. Lei Q, Li Z, Dai C, Wanga J, Chen X, Xie JM, Yang WW, Chen DL. Effect of aluminum on microstructure and property of Cu–Ni–Si alloys, Materials Science & Engineering A. 2013; 572: 65–74.

7. Ilangovan S, SellamuthuR. Effects of tin on hardness, wear rate andcoefficient of friction of cast Cu-Ni-Sn alloys, Journal of Engineering Science and Technology. 2013; 8: 34–43.

8. Li XN, Wang M, Zhao LR, Bao CM, Chu JP, Dong C. Thermal stability of barrierlessCu–Ni–Sn films, Applied Surface Science.2014; 297: 89–94.

9. Zhang Y, Liub P, Tian B, JiaSh, Liu Y. Aging treatment of Cu-Ni-Si-Ag alloy, Procedia Engineering.2012; 27: 1789–1793.

10. Li M,Zinkle SJ. Physical and Mechanical Properties of Copper and Copper Alloys. In: Konings R.J.M., (ed.) Comprehensive Nuclear Materials.2012; 4: 667- 690 Amsterdam: Elsevier.

11. Monteiro WA, Carrio JAG, Da Silveira CR, Vitor E, Buso SJ. Structural and electrical properties of Cu–Ni–Al alloys obtained by conventional powder metallurgy method, Materials Science Forum Vols.2010; 660-66: 41-45.

12. Stobrawa JP,Rdzawski ZM. Precipitation process of the Ni3Al phase in copper-based alloys, Journal of Achievements in Materials and Manufacturing Engineering.2006; 15: 21–26.

13. Stobrawa J. Controlled precipitation in the Cu–Ni–Al based alloys, InzynieriaMaterialowa. 2001; 5: 873-866.

14. Cho Y-R, Kim Y-H, Lee TD. Precipitation hardening and recrystallization in Cu –4% to 7% Ni - 3% Al alloys, J. Mater. Sci.1991; 26: 2879-2886.

15. Deyong L, Tremblay R,Angers R. Microstructural and mechanical properties of rapidly solidified Cu-Ni-Sn alloys, Materials Science and Engineering A. 1990; 124(2): 223-231.

16. Xia CD, Zhang W, Kang ZY, Jia YL, Wu YF, Zhang R, Xu GY, Wang MP. Mater. Sci. Eng. A.2012; 538: 295–301.

17. Akbari-Fakhrabadia A, Mahmudib R, Geranmayehb AR, JamshidijamaM. Mater. Sci. Eng. A.2012; 535: 202–208.

18. Masamichi M, YoshikiyoO. Effects of Co, Ni and Ti additions on the cellular precipitation in Cu-2% Be alloy, Mater. Trans. JIM. 1994; 35 (3): 163–167.

19. Sierpin´ ski Z, GryzieckiJ. Phase transformations and strengthening during ageing of CuNi10Al3 alloy, Mater. Sci. Eng. A. 1999;264: 279–285.

20. Tuck CDS. Langley Alloys, UK, High Strength Copper Nickels.2008.

21. SolimanHN, Hosni HM, RizkA. Effects of physical sputtering and annealing temperature on surface behaviour of Cu-10wt.%Ni alloy, Accepted for publication in Egypt. J. Solids. 2014.

22. Graiss G, Saad G, Fawzy A, Kenawy MA. Gzechoslovak, J. Phys.1991; 41: 149.

23. Habib SK, Rizk A, Mousa IA. Physical parameters affecting deposition rates of binary alloys in a magnetron sputtering system, Vacuum.1998; 49: 153-160.

24. Maniv S, Westwood WD. J. Vac. Sci.Technol.1980; 17: 743.

25. Cullity BD. Elements of X-ray Diffractions, second edition, Addison-Wesley Publishing Company, Inc. 1978;P. 284.

26. Carter G,Colligon JS. Ion Bombardment of Solids, New York, Elsevier. 1968.

27. Lam NQ, JohannessenK.Physical sputtering of Cu-Ni alloys: a molecular dynamics study, Nuclear Instruments and Methods in Physics Research B.1992; 71: 371.

28. Divinski SV, Ribbe J, Schmitz G, HerzigChr.Grain boundary diffusion and segregation of Ni in Cu, ActaMaterialia.2007; 55: 3337-3346.

29. Zhang L, Tang G,Maa X, Russell FM, Cao X,Wang B, Zhang P. Long-range effect of ion irradiation on Cu surface segregation in a CuNi system,Physics Letters A.2011; 375: 1976-1979.

30. Nestorovic S, Milicevic B,MarkovicD. Anneal hardening effect in sintered copper alloys, Science of Sintering. 2002; 34: 169–174.

31. Mao X, Fang F, Yang F, Jiang J, Tan R. Effect of annealing on microstructure and properties of Cu–30Ni alloy tube, Journal of Materials Processing Technology.2009; 209: 2145–2151.